TRANSPLANT INTERNATIONAL

Transplant International ISSN 0934-0874

ORIGINAL ARTICLE

Near-infrared lymphography as a minimally invasive modality for imaging lymphatic reconstitution in a rat orthotopic hind limb transplantation model*

Kate J. Buretta,[1] Gabriel A. Brat,[1] Joani M. Christensen,[1] Zuhaib Ibrahim,[1] Johanna Grahammer,[1] Georg J. Furtmüller,[1] Hiroo Suami,[2] Damon S. Cooney,[1] W. P. Andrew Lee,[1] Gerald Brandacher[1] and Justin M. Sacks[1]

1 Department of Plastic and Reconstructive Surgery, Johns Hopkins University School of Medicine, Baltimore, MD, USA
2 Department of Plastic Surgery, Division of Surgery, University of Texas M.D. Anderson Cancer Center, Houston, TX, USA

Keywords
composite tissue allotransplantation, lymphatics, lymphography, near-infrared, vascularized composite allotransplantation.

Correspondence
Justin M. Sacks MD, FACS, Department of Plastic and Reconstructive Surgery, Johns Hopkins University School of Medicine, 601 North Caroline Street, JHOC 8140D, Baltimore, MD 21287, USA.
Tel.: 443 287 2025;
fax: 410 614 1296;
e-mail: jmsacks@jhmi.edu

Conflicts of interest
Dr. Justin M. Sacks is a speaker and consultant for LifeCell Corporation.

*This study was approved by The Johns Hopkins University Animal Care and Use Committee, protocol #RA11M458. The principles established in 'Guide for the Care and Use of Laboratory Animals, 8th edition,' by the National Research Council of the National Academies, were followed.

Received: 3 March 2013
Revision requested: 7 April 2013
Accepted: 23 June 2013
Published online: 24 July 2013

doi:10.1111/tri.12150

Summary

Wider application of vascularized composite allotransplantation (VCA) is limited by the need for chronic immunosuppression. Recent data suggest that the lymphatic system plays an important role in mediating rejection. This study used near-infrared (NIR) lymphography to describe lymphatic reconstitution in a rat VCA model. Syngeneic (Lewis–Lewis) and allogeneic (Brown Norway–Lewis) rat orthotopic hind limb transplants were performed without immunosuppression. Animals were imaged pre- and postoperatively using indocyanine green (ICG) lymphography. Images were collected using an NIR imaging system. Co-localization was achieved through use of an acrylic paint/hydrogen peroxide mixture. In all transplants, ICG first crossed graft suture lines on postoperative day (POD) 5. Clinical signs of rejection also appeared on POD 5 in allogeneic transplants, with most exhibiting Grade 3 rejection by POD 6. Injection of an acrylic paint/hydrogen peroxide mixture on POD 5 confirmed the existence of continuous lymphatic vessels crossing the suture line and draining into the inguinal lymph node. NIR lymphography is a minimally invasive imaging modality that can be used to study lymphatic vessels in a rat VCA model. In allogeneic transplants, lymphatic reconstitution correlated with clinical rejection. Lymphatic reconstitution may represent an early target for immunomodulation.

Introduction

Transplantation of vascularized composite allografts, including the hand and face, is an increasingly viable reconstructive option for patients suffering major tissue loss unreconstructable by conventional means. Although life-changing, wider application of these operations is limited because of the requirement for chronic immunosuppression and its associated negative sequelae of opportunistic infections, malignancy and systemic toxicity [1,2]. Reducing the requirements for nonspecific systemic immunosuppression and exploring methods of tolerance

induction using cellular and pharmacological therapies is a critical objective of research. Vascularized composite allografts, regardless of current immunosuppressive modalities, experience episodes of rejection, especially of the highly immunogenic skin component [3,4]. To improve clinical outcomes, more information must be gained about the rejection process.

The immunology community has given an increasing amount of attention to the lymphatic system and its role in mediating allograft rejection [5,6]. Studies in skin [7], cardiac [8], islet cell [9], and corneal [6,10] transplant models have indicated that a lymphatic system is critical to the initiation of rejection. In solid organ transplant and limb replantation studies, lymphangiogenesis occurs over a period of several days to weeks [9,11–14] and serves to decrease tissue edema and increase local inflammation by promoting mobilization of macrophages and dendritic cells [15,16]. Once donor lymphatics have anastomosed to recipient lymphatics (lymphatic reconstitution), donor antigen-presenting cells (APCs) expressing alloantigens freely travel to secondary lymph nodes where they initiate alloantigen-specific T cell expansion [17,18]. This direct immune response has been implicated as a primary driver of graft rejection [9,18].

Despite the knowledge that the lymphatic system functions as an immune trafficking highway, little is known about the process of lymphatic reconstitution in vascularized composite allotransplantation (VCA) and whether or not it correlates with graft rejection. Results from solid organ and skin transplant studies cannot be applied to vascularized composite allografts because vascularized composite allografts represent unique immune and tissue environments that include skin, muscle, bone marrow, and secondary lymphoid tissue. Considering the relative immunogenicity of the skin component in a vascularized composite allograft [19] and that cutaneous lymphatics have been shown to reconstitute as early as postoperative day (POD) 4 in limb replant studies [13,20,21], cutaneous lymphatic reconstitution may represent one of the earliest opportunities for effective immunomodulation of vascularized composite allografts, and, as such, warrants further exploration.

Until recently, lymphatic studies were limited owing to the lack of an effective lymphatic imaging modality. Increasingly, researchers are turning to near-infrared (NIR) lymphography as a method for comprehensively studying lymphatics. NIR imaging in the range of 700–900 nm provides deeper penetration into the tissue than visible light and is subject to less scatter and absorption from tissue [22]. NIR lymphography is based on the FDA-approved organic dye, indocyanine green (ICG). ICG is a water-soluble dye that absorbs and emits light with peak wavelengths at 805 and 830 nm, respectively. ICG is administered intradermally, and the subject is imaged in real-time using an NIR laser to track ICG in the body. NIR lymphography has already been used in animal models [23,24] and humans [25] to monitor lymphatic changes in lymphedema models, locate sentinel lymph nodes (SLNs) and draining metastases from tumor beds [26,27], and describe lymphatic architecture in inflammatory models [28,29]. However, no study has directly evaluated the process of lymphatic reconstitution in a VCA model. The aim of our study was to use NIR lymphography to identify collecting lymphatic vessels and characterize cutaneous lymphatic reconstitution in a rat orthotopic hind limb transplant model. We hypothesize that cutaneous lymphatic reconstitution occurs during the post-transplantation acute inflammatory phase and may represent an early immunomodulatory opportunity.

Materials and methods

Animals

Six- to eight-week-old male Brown Norway (BN) and Lewis (LEW) rats were purchased from Harlan Laboratories (Frederick, MD, USA). All rats were housed in a pathogen-free facility. The Institutional Animal Care and Utilization Committee approved the experimental protocol.

Orthotopic hind limb transplantation

Ten LEW rats served as the recipients of syngeneic (LEW to LEW) orthotopic hind limb transplants, while another 10 LEW rats served as the recipients of allogeneic (BN to LEW) orthotopic hind limb transplants. Surgeries were performed as previously described [30]. Briefly, an orthotopic hind limb transplant was performed with osteosynthesis of the femur, approximation of volar and dorsal thigh muscles, and anastomosis of femoral artery and vein. After transplantation, the animals were given 0.05 mg/kg buprenorphine every 12 h through POD 3.

Clinical assessment for lymphangiogenesis and rejection

Transplants were monitored daily during the first postoperative week for clinical signs of rejection based on the previously accepted Banff criteria [31]. Progressive rejection was defined as epidermolysis, desquamation, exudation, eschar formation, and mummification. Frank rejection was defined as clinical progression beyond epidermolysis. Camera images were taken each day during the first 10 PODs to aid in diagnosing clinical rejection as well as to monitor the existence or resolution of clinical lymphedema. After the first 10 days, camera images were taken at the time of euthanasia or on POD 14, whichever occurred first.

To quantitate the severity of edema, thigh circumferences were obtained daily during the first postoperative

week. Each circumference was measured perpendicular to the femur, at a distance halfway between the inguinal crease and the knee. All measurements were performed by the same authors (K.J.B. and G.A.B).

NIR-ICG imaging for normal and transplanted rats

The SPY Elite™ (Novadaq Corporation, Toronto, Canada) NIR imaging device was used to view the rodent lymphatic vessels. The device applies pulses of 805 nm NIR light over a targeted area, causing the administered ICG to fluoresce. Images are captured using a camera with an 830-nm band-pass filter.

Depilation of rats was performed prior to imaging to ensure that hair did not interfere with imaging. Rats were placed under isoflurane sedation anesthesia. ICG (2.5 mg/ml) was injected intradermally into the upper thigh (multiple 2–3 μl injections) using a 30-gauge needle and a micro-injector. Injection sites were 1.5 cm from the graft suture line, at 1.5-cm intervals. At least two ventral sites were chosen for each animal.

After injection of ICG, animals were placed in the supine position, and the hind limb was secured in place. For some imaging sessions, injection sites were covered with tape to limit background fluorescence. Fluorescence images were collected for up to 1 h post injection. Imaging occurred once per day during the first postoperative week and then once per week thereafter.

Co-localization of draining lymphatic vessels

Following euthanasia, rats were injected with a mixture of 3% hydrogen peroxide (97% total volume) and acrylic paint (3% total volume; Prussian blue, green, or orange; Liquitex Artists Materials, Liquitex Professional Acrylic Inc, Piscataway, NJ, USA) at the sites previously used for ICG injection. The injection technique used was similar to that previously described [32]. To directly visualize lymphatic vessels, skin was removed from the inguinal region to the area just distal to the suture line with the assistance of an operating microscope (Leica M620 F20, Leica Microsystems, Inc, Wetzlar GmbH, Germany). In addition, the ipsilateral and contralateral inguinal lymph nodes were harvested and assessed for ICG content using the NIR laser.

Data analysis

To further describe the lymphatic drainage process in this model, a fixed region of interest (ROI) was retrospectively defined along fluorescent lymphatic drainage pathways on fluorescence images. The ROI was selected at an area proximal to the suture line and site of reconstitution but distal to the SLN, or the inguinal node. Using ImageJ (National Institutes of Health, Bethesda, MD, USA), for each transplanted limb, we calculated the mean fluorescence intensity of the ROI at 10, 20, 30, and 60 min post-ICG injection. Injection sites were covered with a dark piece of material to reduce the amount of fluorescence transmitting from the injection site to the ROI.

Results

Clinical and rejection status

Rejection progression was confirmed using visual grading as noted previously. Clinical progression and limb circumference measurements for both transplant groups are summarized in Fig. 1. Syngeneic transplants followed a typical course of clinical edema resolution. Between PODs 4 and 6, limb circumference measurements decreased in 5/6 syngeneic transplants. By POD 7, clinical edema had fully resolved (Fig. 1). The one remaining syngeneic transplant did not experience a notable change in circumference during the first postoperative week. The allogeneic transplants also experienced mild edema PODs 1–4. However, on PODs 5 and 6, the allogeneic transplants experienced a sharp increase in mean limb circumference, which did not resolve before advanced rejection (Banff Criteria Grade 3) was observed on POD 6 or 7 (Fig. 1).

Lymphatic reconstitution in syngeneic transplants

Intradermal injections into the thigh were performed to follow cutaneous lymphatic reconstitution. Preoperatively, intradermal injection of ICG into a native, undisturbed limb immediately resulted in an area of high fluorescence at the injection site. One minute post injection, dye was seen leaving the injection site via multiple fine, linear vessels and draining into the inguinal region (Video Clip S1). Lymphatic drainage of ICG was confirmed through dissection of the ipsilateral and contralateral inguinal lymph nodes and illumination of the nodes with NIR light. Ipsilateral inguinal nodes had green staining from ICG and fluoresced under the NIR light (Fig. 2), whereas the contralateral inguinal nodes lacked green coloration and did not fluoresce.

Compared to native, nontransplanted limbs, ICG was not seen crossing the suture line in 4/4 transplanted limbs imaged PODs 1–4. Instead, the dye pooled in the thigh and remained there for several days. These animals were not imaged again until POD 14. The earliest that ICG was seen crossing the suture line was POD 5. On POD 5, NIR lymphography demonstrated cutaneous lymphatic drainage in 4/6 of the syngeneic transplants imaged. All four animals demonstrating drainage underwent co-localization with the acrylic paint/hydrogen per-

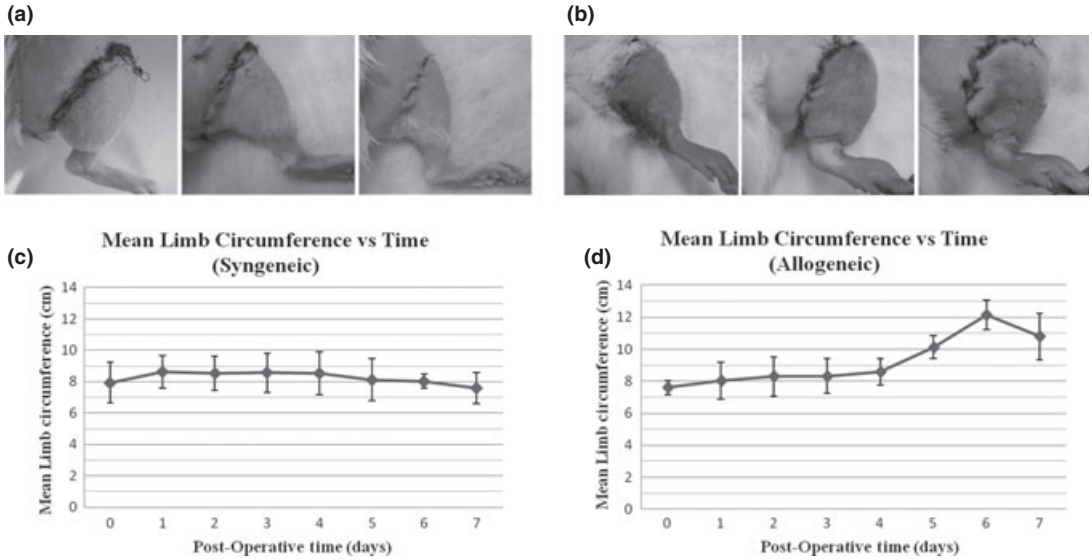

Figure 1 Clinical progression of transplants. (a) Syngeneic transplants experienced clinical edema starting POD 1 (*left*). Edema resolved by POD 5 (*center*) and remained absent on POD 7 (*right*). (b) Allogeneic transplants experienced clinical edema POD 1 (*left*) through sacrifice. POD 5 (*center*). By POD 7, advanced rejection was seen in most animals (Grade 3) (*right*). Depilation was not performed until imaging on POD 5, so as not to induce premature rejection. (c) Quantitative representation of circumference versus time for each syngeneic transplanted limb. (d) Quantitative representation of circumference versus time for each allogeneic transplanted limb. POD, postoperative day.

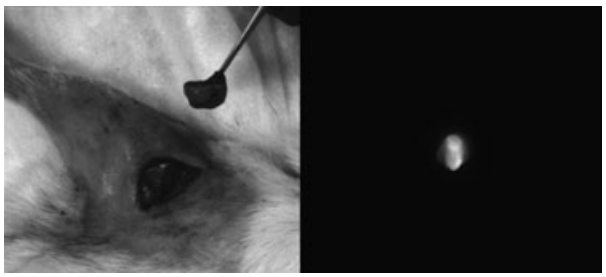

Figure 2 NIR confirmation of lymphatic drainage in a transplant limb. The inguinal node was harvested to confirm ICG drainage via lymphatic vessels into the inguinal node. (*Left*) Inguinal lymph node excision. (*Right*) NIR image showing fluorescence of the inguinal node. NIR, near-infrared; ICG, indocyanine green.

oxide mixture method. By POD 7, the remaining two syngeneic transplants demonstrated drainage. By POD 14, multiple tortuous vessels were seen crossing the suture line in all transplants imaged (Fig. 3).

Lymphatic reconstitution in allogeneic transplants

Prior to transplantation, NIR lymphography of native BN limbs demonstrated multiple, discrete vessels draining dye into the inguinal region. This pattern was similar to that seen in the preoperative syngeneic hind limb transplant model. NIR lymphography demonstrated ICG pooling without drainage through POD 4 in 4/4 allogeneic transplants. These animals were not imaged again. POD 5 was the first day that ICG was seen crossing the suture line. On POD 5, 4/6 allogeneic transplants demonstrated cutaneous drainage (Fig. 4). With two transplants, ICG was never visualized crossing the suture line before advanced rejection set in. By the end of POD 5, all allogeneic transplants that had undergone imaging (6/6) demonstrated at least Grade 2 clinical rejection (as shown in Fig. 1), with 2/6 demonstrating Grade 3 advanced clinical rejection. By POD 7, 5/6 allogeneic transplants demonstrated Grade 3 rejection (as shown in Fig. 1). Limbs were edematous and continued to grow in diameter until the tissues began to necrose. In line with advanced rejection, on POD 7, ICG pooled in all transplanted limbs (6/6) and was not visualized crossing the suture line (Fig. 4). By the end of POD 10, all allogeneic transplant recipients had been sacrificed owing to Grade 4 rejection.

Real-time imaging of lymphatic drainage

A typical drainage pattern was seen over a 60-min imaging session for rats demonstrating cutaneous lymphatic reconstitution (Fig. 5). Over time, an increasing amount of dye was transported across the suture line as evidenced by an increase in the number of lymphatic vessels visualized. In addition, fluorescent intensities were measured for a retrospectively chosen ROI between the suture line and draining inguinal node at 1, 5, 10, 20, 30, and 60 min post injection.

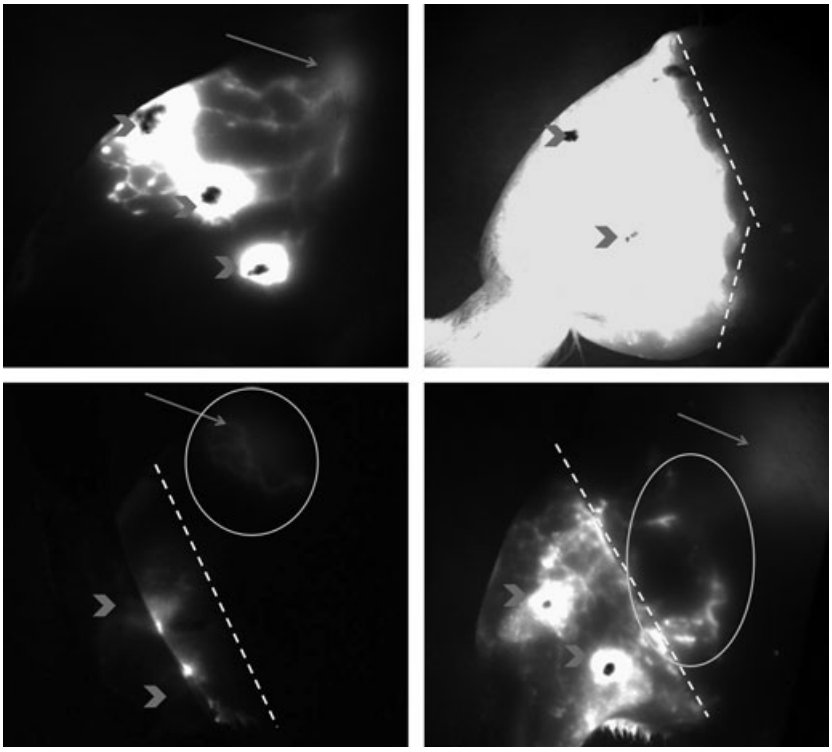

Figure 3 Lymphatic drainage in syngeneic hind limb transplants. Ventral view. (*Top, left*) Preoperative NIR lymphography showing lymphatic drainage of donor hind limb to the inguinal region (red arrow). Injection sites: arrowheads. (*Top, right*) POD 4. Lymphatic drainage remained disrupted. Dye did not pass the suture line (dashed line). (*Bottom, left*) POD 5. Lymphatic reconstitution. ICG was seen crossing the suture line via lymphatic vessels (circle) and draining into the inguinal node region (arrow). (*Bottom, right*) POD 14. Further lymphatic reconstitution. NIR, near-infrared; POD, postoperative day; ICG, indocyanine green.

The mean fluorescence intensity increased steadily over the 60-min imaging session.

Confirmation and co-localization of ICG imaging with anatomic dissection

Immediately upon intradermal injection of the acrylic paint–hydrogen peroxide mixture, a large bubble formed under the skin as oxygen was released from the hydrogen peroxide. Within the dermis, the paint moved quickly into the lymphatic vessels and tracked to the inguinal node in an anterograde fashion. Upon dissection, discrete, paint-stained lymphatic vessels could be seen traversing the suture line and draining into the inguinal lymph node as early as POD 5 in 3/4 of the syngeneic transplants and 2/4 of the allogeneic transplants that had demonstrated drainage via NIR imaging (Fig. 6). Lymphatic vessels were distinguished by their pale, thin vessel walls and visible valves.

Discussion

Although ICG-based NIR lymphography has been used for multiple applications, our study is the first to directly address lymphatic reconstitution. This study has shown that ICG-based NIR lymphography is an effective, clinically translatable imaging modality for studying lymphatic reconstitution in a rat orthotopic hind limb transplantation model. Until recently, lymphoscintigraphy was the main modality used for intra-lymphatic imaging. Although lymphoscintigraphy has been used successfully to diagnose lymphedema and locate SLNs [33], this technique is time consuming, impractical for *in vivo* imaging [34], and suffers from poor spatial resolution [24,35]. To appropriately identify lymphatic collecting vessels and quickly characterize how and when major histocompatibility complex-mismatched tissues recreate lymphatic connections, an imaging modality is needed that provides rapid, nontoxic *in vivo* imaging of lymphatic vessels as fine as those found in the dermis. Empiric, phantom, and theoretical studies have shown that NIR lymphography has good resolution in biologic tissues up to 6 mm deep [36]. As a result, we were able to image discrete dermal lymphatic vessels traversing transplant suture lines and draining into ipsilateral inguinal lymph nodes. Analyzing these data, we were able to discern lymphedema patterns and determine the temporal relationships by which

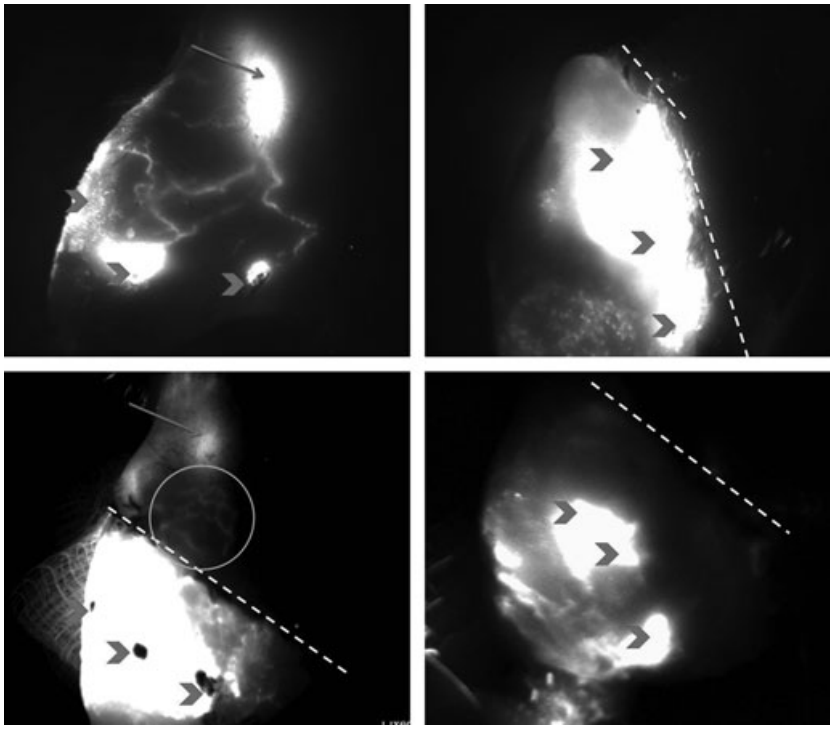

Figure 4 Lymphatic drainage in allogeneic hind limb transplants. Ventral view. (*Top, left*) Preoperative NIR lymphography showing lymphatic drainage of donor hind limb to the inguinal node (arrow). ICG injection sites (arrow heads). (*Top, right*) POD 2. Cutaneous lymphatic drainage is disrupted as no dye passes the suture line (dashed line). (*Bottom, left*) POD 5. Lymphatic reconstitution. ICG first crossed the suture line on POD 5 via new lymphatic vasculature (green circle) and drained into the inguinal node (arrow). (*Bottom, right*) POD 7. Cutaneous lymphatic drainage is again disrupted, and no dye crosses the suture line. NIR, near-infrared; ICG, indocyanine green; POD, postoperative day.

orthotopic hind limb transplants first reconstitute cutaneous lymphatic drainage.

Our model demonstrated fluid drainage and lymphedema resolution patterns similar to previously published replant and VCA data. As shown before [37], we saw pooling of the ICG dye at the wound site immediately after lymphatic vessel disruption. In accordance with the replant literature [13,20,21,38], we found that by POD 5, fluid drainage of the surgically altered hind limb is sufficient to decrease postoperative edema, as measured by circumference changes and clinical assessment. Confirming of our hypothesis, this coincided with the ability to visualize lymphatic channels using ICG-based NIR imaging. However, noting this correlation, we do not discount the effect that venous regeneration may have had on the resolution of clinical edema. In addition, consistent with prior ICG lymphography data, our intensity data show that ICG drains in a time-dependent manner as indicated by increases in mean fluorescence intensity over time for draining lymphatic vessels (Fig. 5) [39]. Of note, some transplanted limbs were significantly less edematous PODs 2–4 and required less time to establish drainage of ICG than others. We attribute these differences to variations in the amount of edema and inflammation between rats, possibly because of differences in surgical ischemia time and/or reperfusion injury. Overall, however, two distinctly different edema patterns emerged between the syngeneic and allogeneic transplants during the first postoperative week (Fig. 1), suggesting that variations in ischemia time and reperfusion injury contributed to clinical edema less than graft rejection.

Reconstitution of lymphatic drainage was first described in the replant literature. Evidence of lymphatic reconstitution was seen in rat hind limb replant models as early as POD 4 [13,20,21] and in canine replant models as early as POD 7 [40]. These studies were all done using a lymphatic imaging method other than NIR imaging. As mentioned previously, our findings are consistent with data from the replantation literature gained from lymphoscintographic techniques. However, our findings are different from recent studies of cutaneous reconstitution as assessed by ICG-based NIR lymphography [11,41]. These studies, which used skin graft and tail ligation models, did not see noninterstitial cutaneous lymphatic flow across disrupted cutaneous tissue until 2–6 weeks post operation. We hypothesize that the discrepancy may be caused by the inclusion of

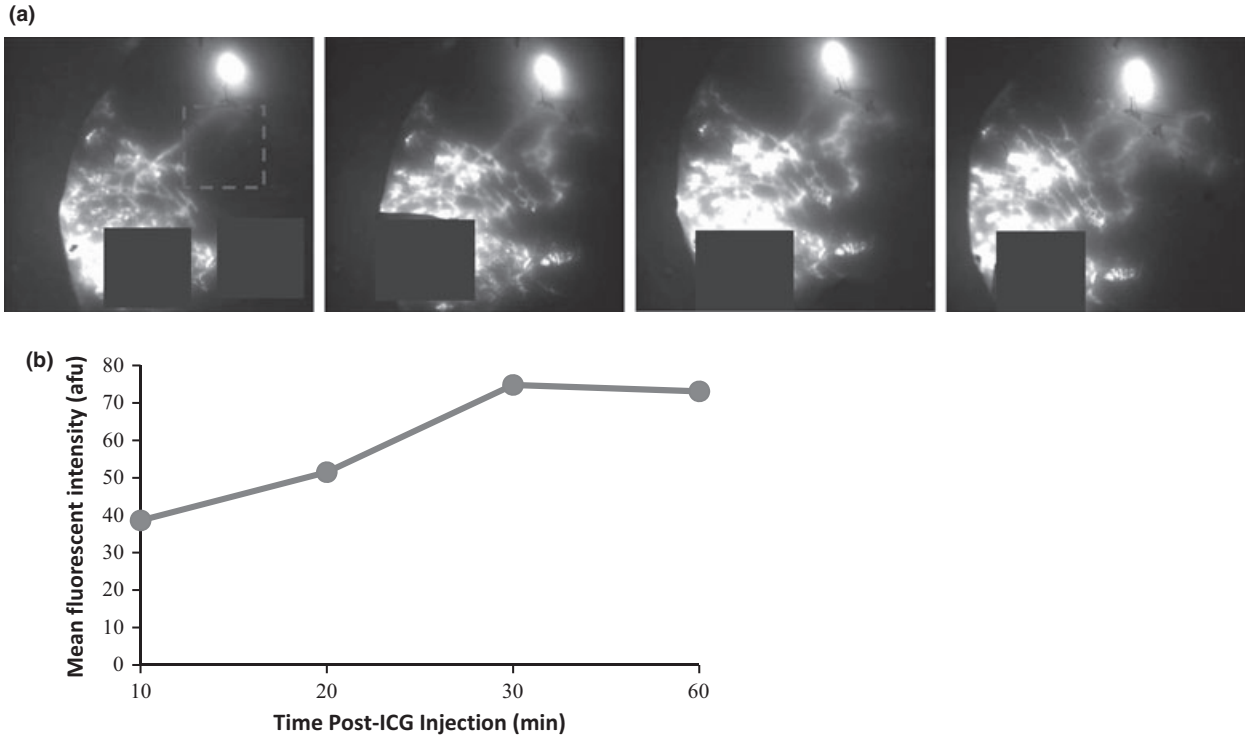

Figure 5 Real-time assessment of lymphatic drainage. (a) NIR images of lymphatic drainage showing the progression of flow at 10 (*far left*), 20 (*second from left*), 30 (*second from right*), and 60 (*far right*) min post-ICG injection. The solid boxes are covering injection sites. A region of interest (ROI) was selected for measurements of fluorescent intensity (dashed box). The same ROI was measured for each image. (b) Graph depicting the mean fluorescent intensity of the ROI versus time post-ICG injection. NIR, near-infrared; ICG, indocyanine green.

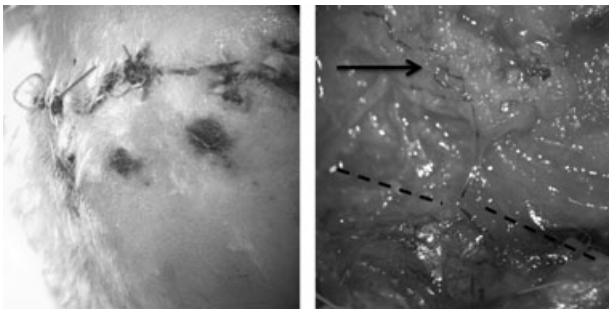

Figure 6 Confirmation and co-localization of ICG imaging. A blue acrylic paint/hydrogen peroxide mixture injected near the previous ICG injection locations (*left*) demonstrated discrete lymphatic vessels crossing the suture line (dashed line) and draining into the inguinal node region (arrow) on POD 5 (*right*). ICG, indocyanine green.

secondary lymphoid tissue in our orthotopic hind limb transplants, which may serve to promote lymphangiogenesis [42,43]. Furthermore, transplantation of a full hind limb provides a structurally intact lymphatic system for recipient tissues to co-apt and anastomose.

In addition, our findings vary from the only other study that examined lymphatic drainage in vascularized composite allografts [44]. In this study, NIR lymphography of non-human primate heterotopic facial allografts revealed that nonsuperficial cutaneous lymphatic drainage of the graft, as assessed by edema patterns, did not improve until 2 weeks post operation. Notably, the authors employed a subcutaneous injection technique, which may have led to inadequately imaged cutaneous lymphatics. In addition, a heterotopic model was used instead of an orthotopic model. Our early visualization of lymphatic channels prompted us to employ subsequent techniques to ensure that the channels identified were truly lymphatic vessels. We harvested the inguinal node post lymphography to ensure that dye had traveled to a secondary lymphoid tissue and injected acrylic paint to confirm the lymphatic channels our dye had used to reach those nodes.

In the allogeneic transplant group, visualization of lymphatic channels on POD 5 correlated with both advanced rejection by POD 6 or 7 [45,46] and significant disruption of lymphatic flow once the limb had progressed to advanced rejection [44]. Our findings indicate that cutaneous lymphatic reconstitution occurs in parallel with the acute inflammatory period after hind limb transplantation. This finding is consistent with the landmark 1968 study by Barker and Billingham, which showed that mechanical prevention of lymphatic reconstitution in a

skin allograft reduced the graft's antigenicity and allowed for indefinite graft survival [7]. Building off this knowledge, researchers in the 1970–1990 studied the use of thoracic duct drainage (TDD) as an adjunct to standard immunosuppressive therapies for organ transplantation [47–51]. TDD was initiated in the recipient prior to transplantation in the hopes of decreasing the number of circulating lymphocytes that able to initiate an acute rejection episode. Although long-term data did not show an obvious benefit of TDD plus standard immunosuppressive therapy versus standard immunosuppressive therapy alone [49], studies were able to show that the addition of TDD increased the likelihood of graft survival in the first few years post transplantation [48].

Decades later, we know that blocking lymphatic drainage prevents donor skin APCs from presenting alloantigen to naive T cells in draining lymph nodes [52]. Although other mechanisms of rejection have been identified [53–55], this pathway is dominant in the skin. Similar to the authors that studied skin graft drainage and TDD, it is our thought that attenuating lymphatic drainage, particularly cutaneous lymphatic drainage, early in the post-transplantation period may decrease the load of APCs traveling between the donor and recipient of vascularized composite allografts. Transient interruption of the direct immune response may allow for alternate antigen presentation pathways to shift immune activity toward an immunomodulating cell response and thus improve short-term graft survival. In conjunction with today's improved immunosuppressive therapies, attenuation of lymphatic drainage may have a larger, and more lasting, effect on overall allograft survival than in the TDD studies.

This study provided confirmation of our ability to rapidly image cutaneous lymphatics, established a timeline for cutaneous lymphatic reconstitution in our transplant model, and correlated clinical rejection with lymphatic reconstitution. Cutaneous and deep lymphatics reorganize post transplant and potentially initiate the acute inflammatory response. These concepts represent fertile areas of investigation for the immunomodulation of vascularized composite allografts. In future studies, we hope to better elucidate the mechanisms of immune cell trafficking through the lymphatic vessels imaged by our techniques and further explore the unique role cutaneous lymphatic drainage plays in allograft rejection. With an increased understanding of the timing during which the lymphatic system reconstitutes and the mechanics behind antigen presentation within the system, we can fashion modalities to potentially modify the process of rejection in vascularized composite allografts. Examples of such modifications include using photodynamic therapy or immunosuppressive medications to ablate or slow the reconstitution of cutaneous lymphatics and thus delay antigen presentation.

A major limitation of this study was the small time window between POD 5 and POD 6 during which lymphatic vessels could be seen bridging the suture line in most allogeneic transplants. Prior to POD 5, vessels were not visualized in any of the transplanted limbs, and by the end of POD 6, discrete lymphatic vessels could no longer be visualized and dye did not drain to the ipsilateral inguinal node. This discontinuation of drainage occurred at the same time that allogeneic transplants exhibited clinical signs of advanced rejection. The small time frame between reconstitution and advanced rejection makes sense in our study because once reconstitution occurs, there is presumably a large amount of APCs suddenly able to travel between the donor and recipient. Rapid degeneration of lymphatic vessels shortly after reconstitution may have contributed to our inability to visualize ICG crossing the suture line in 2/6 allogeneic transplants on POD 5. In addition, variations in ischemia time and/or reperfusion injury may have led to increased inflammation and edema in the transplants, obscuring our view of the lymphatics. Other limitations include primarily focusing on cutaneous lymphatic vessels without full evaluation of deeper lymphatic channels and not discerning how much of the lymphatic flow was interstitial versus intralymphatic. This study did not assess the effect of immunosuppression on the lymphatic reconstitution process. Finally, as this was a preliminary feasibility study, further studies with larger subject numbers are warranted.

Sequential NIR fluorescent imaging of rat orthotopic hind limb transplants demonstrated that, in both syngeneic and allogeneic rat orthotopic hind limb transplants, lymphatic reconstitution occurs during the acute inflammatory phase. Lymphatic reconstitution may play an important role in the acute rejection of vascularized composite allografts and may thus serve as an early target for immunomodulation. ICG-based NIR lymphography is a noninvasive imaging modality that may be particularly useful for further exploration of this relationship and, potentially, immune status monitoring of vascularized composite allografts. Other applications for ICG-based NIR lymphography, some of which have already been initiated, include: determining the association between lymphatic drainage and tracking of cellular responses in the skin, identification of changing reconstitution characteristics for different cutaneous tissues without the need for biopsy, correlating different drug regimes with dynamic lymphatic changes, and dynamic destruction of lymphatic vasculature in an attempt to prevent inflammation.

Authorship

KJB, GAB and JMS: designed the study, collected and analyzed data, wrote and revised the paper. JMC: collected and

analyzed data, revised the paper. ZI, JG and GJF: collected data. HS and WPAL: designed the study and revision of paper. DSC and GB: designed the study, analyzed data, and revision of paper.

Funding

This study was funded by an unrestricted educational grant from Novadaq Inc.

Acknowledgements

Special thanks to Robert Flower, PhD, for his invaluable insight into NIR imaging.

Supporting Information

Additional Supporting Information may be found in the online version of this article:

Video Clip S1. Real-time drainage of ICG from a transplanted rat hind limb. (*Ventral view*) ICG can be seen draining from the skin of the transplanted hind limb into the ipsilateral inguinal node (*bright circular region on the right side of the image*) of the recipient via the contraction of fine lymphatic vessels. The ICG injection site is covered to limit the amount of nonspecific fluorescence seen in the inguinal region.

References

1. Petit F, Minns AB, Dubernard J-M, Hettiaratchy S, Lee WPA. Composite tissue allotransplantation and reconstructive surgery: first clinical applications. *Ann Surg* 2003; **237**: 19.
2. Hettiaratchy S, Randolph MA, Petit F, Lee WPA, Butler PEM. Composite tissue allotransplantation – a new era in plastic surgery? *Br J Plast Surg* 2004; **57**: 381.
3. Shores JT, Imbriglia JE, Lee WPA. The current state of hand transplantation. *J Hand Surg* 2011; **36**: 1862.
4. Sacks JM, Horibe EK, Lee WPA. Cellular therapies for prolongation of composite tissue allograft transplantation. *Clin Plast Surg* 2007; **34**: 291.
5. Bromberg JS, Heeger PS, Li XC. Evolving paradigms that determine the fate of an allograft. *Am J Transplant* 2010; **10**: 1143.
6. Dietrich T, Bock F, Yuen D, *et al.* Cutting edge: lymphatic vessels, not blood vessels, primarily mediate immune rejections after transplantation. *J Immunol* 2010; **184**: 535.
7. Barker C, Billingham R. The role of afferent lymphatics in the rejection of skin homografts. *J Exp Med* 1968; **128**: 197.
8. Nykänen AI, Sandelin H, Krebs R, *et al.* Targeting lymphatic vessel activation and CCL21 production by vascular endothelial growth factor receptor-3 inhibition has novel immunomodulatory and antiarteriosclerotic effects in cardiac allografts. *Circulation* 2010; **121**: 1413.
9. Yin N, Zhang N, Xu J, Shi Q, Ding Y, Bromberg JS. Targeting lymphangiogenesis after islet transplantation prolongs islet allograft survival. *Transplantation* 2011; **92**: 25.
10. Yuen D, Pytowski B, Chen L. Combined blockade of VEGFR-2 and VEGFR-3 inhibits inflammatory lymphangiogenesis in early and middle stages. *Invest Ophthalmol Vis Sci* 2011; **52**: 2593.
11. Yan A, Avraham T, Zampell JC, Aschen SZ, Mehrara BJ. Mechanisms of lymphatic regeneration after tissue transfer. *PLoS ONE* 2011; **6**: e17201.
12. Uner A, Weinberg AM, Nautrup CP, *et al.* Spontaneous reanastomosis between lymphatic vessels following syngeneic transplantation of the small intestine in the rat. *Surg Radiol Anat* 2001; **23**: 383.
13. Kramer EL, McLaws R, Sanger JJ, Shaw W. Lymphedema in the replanted limb of the rat: scintigraphic evaluation. *Microsurgery* 1985; **6**: 40.
14. Källskog O, Kampf C, Andersson A, *et al.* Lymphatic vessels in pancreatic islets implanted under the renal capsule of rats. *Am J Transplant* 2006; **6**: 680.
15. Baluk P, Tammela T, Ator E, *et al.* Pathogenesis of persistent lymphatic vessel hyperplasia in chronic airway inflammation. *J Clin Invest* 2005; **115**: 247.
16. Kataru RP, Jung K, Jang C, *et al.* Critical role of CD11b+ macrophages and VEGF in inflammatory lymphangiogenesis, antigen clearance, and inflammation resolution. *Blood* 2009; **113**: 5650.
17. Cursiefen C, Chen L, Dana MR, Streilein JW. Corneal lymphangiogenesis transplant immunology. *Cornea* 2003; **22**: 273.
18. Morelli AE, Larregina AT. Apoptotic cell-based therapies against transplant rejection: role of recipient's dendritic cells. *Apoptosis* 2010; **15**: 1083.
19. Lee W, Yaremchuk M, Pan Y-C, Randolph M, Tan C, Weiland A. Relative antigenicity of components of a vascularized limb allograft. *Plast Reconstr Surg* 1991; **87**: 401.
20. Reichert F. The regeneration of the lymphatics. *Arch Surgery* 1926; **13**: 871.
21. Anthony J, Foster R, Price D. Lymphatic regeneration following microvascular limb replantation: a qualitative and quantitative animal study. *J Reconstr Microsurg* 1997; **13**: 327.
22. Portnoy E, Lecht S, Lazarovici P, Danino D, Magdassi S. Cetuximab-labeled liposomes containing near-infrared probe for *in vivo* imaging. *Nanomedicine: NBM* 2011; **xx**: 1.
23. Mäkinen T, Jussila L, Veikkola T, *et al.* Inhibition of lymphangiogenesis with resulting lymphedema in transgenic mice expressing soluble VEGF receptor-3. *Nat Med* 2001; **7**: 199.
24. Ogata F, Azuma R, Kikuchi M, Koshima I, Morimoto Y. Novel lymphography using ndocyanine green dye for near-infrared fluorescence labeling. *Ann Plast Surg* 2007; **58**: 652.

25. Unno N, Nishiyama M, Suzuki M, *et al.* Quantitative lymph imaging for assessment of lymph function using indocyanine green fluorescence lymphography. *Eur J Vasc Endovasc Surg* 2008; **36**: 230.
26. Tagaya N, Aoyagi H, Nakagawa A, *et al.* A novel approach for sentinel lymph node identification using fluorescence imaging and image overlay navigation surgery in patients with breast cancer. *World J Surg* 2011; **35**: 154.
27. Crane LM, Themelis G, Buddingh KT, *et al.* Multispectral real-time fluorescence imaging for intraoperative detection of the sentinel lymph node in gynecologic oncology. *JoVE* 2010; **pii**: 2225.
28. Zhou Q, Wood R, Schwarz E, Wang Y-J, Xing L. Near infrared lymphatic imaging demonstrates the dynamics of lymph flow and lymphangiogenesis during the acute vs. chronic phases of arthritis in mice. *Arthritis Rheum* 2011; **62**: 1881.
29. Guo R, Zhou Q, Proulx ST, *et al.* Inhibition of lymphangiogenesis and lymphatic drainage via vascular endothelial growth factor receptor 3 blockade increases the severity of inflammation in a mouse model of chronic inflammatory arthritis. *Arthritis Rheum* 2009; **60**: 2666.
30. Sacks JM, Kuo Y-R, Horibe EK, *et al.* An optimized dual-surgeon simultaneous orthotopic hind-limb allotransplantation model in rats. *J Reconstr Microsurg* 2012; **28**: 69.
31. Cendales LC, Kanitakis J, Schneeberger S, *et al.* The Banff 2007 working classification of skin-containing composite tissue allograft pathology. *Am J Transplant* 2008; **8**: 1396.
32. Suami H, Chang DW, Matsumoto K, Kimata Y. Demonstrating the lymphatic system in rats with microinjection. *Anat Rec* 2011; **294**: 1566.
33. Sharma R, Wendt JA, Rasmussen JC, Adams KE, Marshall MV, Sevick-Muraca EM. New horizons for imaging lymphatic function. *Ann N Y Acad Sci* 2008; **1131**: 13.
34. Yamamoto T, Narushima M, Doi K, *et al.* Characteristic indocyanine green lymphography findings in lower extremity lymphedema: the generation of a novel lymphedema severity staging system using dermal backflow patterns. *Plast Reconstr Surg* 2011; **127**: 1979.
35. Barrett T, Choyke PL, Kobayashi H. Imaging of the lymphatic system: new horizons. *Contrast Med Mol Imaging* 2006; **245**: 230.
36. Weiler M, Kassis T, Dixon JB. Sensitivity analysis of near-infrared functional lymphatic imaging. *J Biomed Opt* 2012; **17**: 066019-1.
37. Mendez U, Brown EM, Ongstad EL, Slis JR, Goldman J. Functional recovery of fluid drainage precedes lymphangiogenesis in acute murine foreleg lymphedema. *Am J Physiol Heart Circ Physiol* 2012; **302**: H2250.
38. Danese C, Howard JM, Bower R. Regeneration of lymphatic vessels: a radiographic study. *Ann Surg* 1962; **156**: 61.
39. Kwon S, Sevick-Muraca EM. Noninvasive quantitative imaging of lymph function in mice. *Lymphatic Res Biol* 2007; **5**: 219.
40. Smaropoulos EC, Papazoglou LG, Patsikas MN, Vretou E, Petropoulos AS. Lymphatic regeneration following hind limb replantation: an experimental study in the dog. *Eur J Pediatr Surg* 2005; **15**: 337.
41. Slavin SA, Van den Abbeele AD, Losken A, Swartz MA, Jain RK. Return of lymphatic function after flap transfer for acute lymphedema. *Ann Surg* 1999; **229**: 421.
42. Becker C, Assouad J, Riquet M, Hidden G. Postmastectomy lymphedema: long-term results following microsurgical lymph node transplantation. *Ann Surg* 2006; **243**: 313.
43. Blum KS, Hadamitzky C, Gratz KF, Pabst R. Effects of autotransplanted lymph node fragments on the lymphatic system in the pig model. *Breast Cancer Res* 2010; **120**: 59.
44. Mundinger GS, Narushima M, Hui-Chou HG, *et al.* Infrared fluorescence imaging of lymphatic regeneration in nonhuman primate facial vascularized composite allografts. *Ann Plast Surg* 2012; **68**: 314.
45. Sucher R, Lin C-H, Zanoun R, *et al.* Mouse hind limb transplantation: a new composite tissue allotransplantation model using nonsuture supermicrosurgery. *Transplantation* 2010; **90**: 1374.
46. Zhang Z, Dong H, Meng L, *et al.* A modified rat model of acute limb allograft rejection. *Transplant Proc* 2011; **43**: 3987.
47. Starzl TE, Weil R, Koep LJ, *et al.* Thoracic duct fistula and renal transplantation. *Ann Surg* 1979; **190**: 474.
48. Fish JC, Sarles HE, Remmers A, Townsend CM. Renal transplantation after thoracic duct drainage. *Ann Surg* 1980; **193**: 752.
49. Kinukawa T, Ono Y, Takeuchi N, Ohshima S. Analysis of long-term results in kidney transplantation performed using a rejection-free protocol with cyclosporine and thoracic duct drainage. *Transplant Proc* 1997; **29**: 946.
50. Fish JC, Flye MW, Williams A, *et al.* Inability of thoracic duct drainage to prevent hyperacute rejection. *Transplantation* 1983; **36**: 134.
51. Laville M, Cordier G, Brochier J, Lefebvre R, Revillard JP, Traeger J. Improvement of cadaveric renal allograft survival by thoracic duct drainage: relation with T-lymphocyte subset modifications assessed by flow-cytometry. *Proc Eur Dial Transplant Assoc* 1983; **19**: 488.
52. Teoh D, Johnson LA, Hanke T, McMichael AJ, Jackson DG. Blocking development of a CD8+ T cell response by targeting lymphatic recruitment of APC. *J Immunol* 2009; **182**: 2425.
53. Celli S, Albert ML, Bousso P. Visualizing the innate and adaptive immune responses underlying allograft rejection by two-photon microscopy. *Nat Med* 2011; **17**: 744.
54. Yamanokuchi S, Ikai I, Nishitai R, *et al.* Asialo GM1 positive CD8+ T cells induce skin allograft rejection in the absence of the secondary lymphoid organs. *J Surg Res* 2005; **129**: 57.
55. Llodrá J, Angeli V, Liu J, Trogan E, Fisher EA, Randolph GJ. Emigration of monocyte-derived cells from atherosclerotic lesions characterizes regressive, but not progressive, plaques. *Proc Natl Acad Sci U S A* 2004; **101**: 11779.

